

Linear Galerkin-Legendre spectral scheme for a degenerate nonlinear and nonlocal parabolic equation arising in climatology

Łukasz Płociniczak^{*,†}

Abstract

A special place in climatology is taken by the so-called conceptual climate models. These, relatively simple, sets of differential equations can successfully describe single mechanisms of the climate. We focus on one family of such models based on the global energy balance. This gives rise to a degenerate nonlocal parabolic nonlinear partial differential equation for the zonally averaged temperature. We construct a fully discrete numerical method that has an optimal spectral accuracy in space and second order in time. Our scheme is based on Galerkin formulation of the Legendre basis expansion which is particularly convenient for this setting. By using extrapolation the numerical scheme is linear even though the original equation is strongly nonlinear. We also test our theoretical result during various numerical simulations that confirm the aforementioned accuracy of the scheme. All implementations are coded in Julia programming language with the use of parallelization (multi-threading).

Keywords: spectral method, climate dynamics, degenerate equation, nonlocal operator, fractional integral, parabolic equation

AMS Classification: 35K65, 35K55, 65M70, 86A08

1 Introduction

In climate dynamics one distinguishes between various models according to their complexity and number of physically resolved phenomena. Overall, there is a hierarchy of models in which on the one end we have General Circulation Models (GCMs), and on the other - Conceptual Climate Models [12, 65, 68, 66, 72, 49]. In between there are Models of Intermediate Complexity that frequently utilize coarser grids or a larger number of parametrizations of various phenomena than GCMs [10]. General Circulation Models are the most advanced descriptions of the global flow of the planetary atmosphere or ocean along with many physical quantities such as pressure, temperature, and water vapour to name only a few. Because they are systems of nonlinear partial differential equations to be solved for long times on a sphere, they usually require supercomputers to analyse and resolve. Thanks to that they are used to gain quantitative insight about the various interactions between different constituents of the Earth system. Moreover, they are crucial in making predictions of different scenarios concerning, for instance, greenhouse gas emissions and their impact on the mean temperature [11].

^{*}Faculty of Pure and Applied Mathematics, Wrocław University of Science and Technology, Wyb. Wyspiańskiego 27, 50-370 Wrocław, Poland

[†]Email: lukasz.plociniczak@pwr.edu.pl

On the other side of the spectrum are Conceptual Climate models that usually are low-order dynamical systems. Their role is to describe several mechanisms of the climate along with their nonlinear interdependencies rather than simulate the whole Earth system. They are very useful to investigate steady-states of the climate and their bifurcations which might be difficult to resolve in the full GCMs. For example, conceptual climate models may only focus on energy balance to describe the global or zonally (longitudinally) averaged temperature and steady states of the climate that arise from it. The seminal works concerning this concept have been done by Budyko [6], Sellers [70] for zero-dimensional case (global mean) and North [52, 53, 55] for meridional evolution of the temperature (zonal mean). Overall, in the energy balance models one usually assumes that the temperature distribution $T = T(x, t)$, where x denotes the sine of the latitude, is governed by the incoming solar radiation, outgoing infrared radiation, and some mechanism of horizontal (meridional) energy transport. Further, as was first noted in [5] the reflectivity of the surface may depend on the history of the temperature. This leads to a nonlinear and nonlocal parabolic equation that is the main subject of our investigations

$$\begin{cases} T_t = (d(T)(1 - x^2)T_x)_x + g(x, t, T, JT), & x \in (0, 1), \quad t > 0, \\ T_x(0, t) = 0, \quad T_x(1, t) < \infty, \\ T(x, s) = T_0(x, s), & -\tau \leq s \leq 0, \end{cases} \quad (1)$$

where the nonlocal (memory) operator with a kernel K is defined as

$$JT(x, t) = \int_0^\tau K(s)T(x, t - s)ds. \quad (2)$$

Here, $d = d(T)$ is the possibly nonlinear diffusivity while g is the nonlinear source term. Notice that the nonlocality enters the equation through the latter and the second order differential operator is degenerate for $x = 1$. A derivation of the above model in the framework of climate dynamics is given in the next section. In early works the model was analysed from the climatological point of view in [51] where the natural efficiency of Legendre orthogonal polynomials was noticed. The linear case was solved exactly for several first modes while the nonlinear one, with the diffusivity proportional to the flux as proposed in [73], iteratively in [42]. In this work author noted that nonlinear effects have a significant impact on the sensitivity of the model to variations in the solar constant. Moreover, due to a nonlinear source, which is a consequence of the ice-albedo feedback discussed below, the equation can have several steady-states representing different climates. Their stability, bifurcations, and sensitivity to parameter perturbations is of high importance in climatology. Previously cited papers also deal with this issue and some further results can be found in [31, 41]. The simple energy balance model has been generalized in several ways by adding additional degrees of freedom. For the globally averaged model one can mention adding a mass balance to account for ice sheet variations [37, 28, 61, 62] or the amount of CO_2 in the atmosphere [26, 25]. This is especially relevant for understanding oscillations of ice ages and their rhythmicity. Further information concerning this topic can be found in [46, 12, 22, 56, 63, 14, 78]. A modern review of decades of research on energy balance models can be found in a readable book of North and Kim [55].

There is also a broad literature concerning mathematical aspects of the above problem. Its existence, uniqueness, and regularity of solutions was investigated by Hetzer in [33, 34]. Moreover, an essential problem for applications - parameter estimation - was analysed in [67, 7]. As was noted above, steady-states of the problem can bifurcate what can lead to hysteresis. Mathematical analysis of this phenomenon was given in [18, 32]. Some other interesting results concerning the local version of the model were obtained by Diaz [16] where the general mathematical theory of energy balance models has been developed for a possibly degenerate nonlinear diffusivity. Further, a generalization of the equation on the 2-sphere into a Riemannian manifold without the boundary was analysed in [4] where also a numerical treatment was conducted. Furthermore, since in some

parametrizations the source can exhibit a discontinuity in the temperature, a free-boundary can arise. We give a climatological background of this phenomenon in the next section and the reader can consult [19, 17, 83] for a thorough treatment. Some other generalizations consist of stochastic terms [20], including continent distribution [35], and solving inverse problem [77]. We also would like to mention broad studies conducted from the dynamical systems point of view in which the horizontal transport is modelled by a relaxation term for the globally averaged temperature [47, 48, 80, 79, 82].

There are several accounts of numerical treatment of energy balance models. The early simulations were based on spectral Legendre decomposition in space and the first order implicit Euler scheme in time [54]. As was also noted in [52] the model is amenable for such a treatment due to rapid convergence of the orthogonal series. Recently, several papers concerning finite element method were published. In [4, 3] the situation set on a two-dimensional Riemannian manifold was solved in the case of nonlinear diffusivity modelled by a p-Laplacian. On the other hand, in [35] a finite volume WENO method has been applied to solve the problem where the surface of the Earth is split into land and ocean fractions. Similar analysis but with emphasis on equilibrium solutions was given in [36]. Since our model involves a nonlocal operator we would also like to point the interested reader to a expository literature concerning these [2, 21, 43, 40]

In this paper we design and analyse a two-step spectral method based on the Galerkin-Legendre approximation that is weighted in time. In particular our method contains the second order in time Crank-Nicolson scheme. The main motivation of this paper is to present a rigorous convergence treatment of the early ideas of energy balance simulations [54]. Spectral methods are known for their exponential accuracy provided the regularity of the solution. This can significantly reduce the computation time since only a small number of terms in the expansion needs to be calculated. This is especially relevant for dealing with nonlocal operators that require all the information about the history in each time-stepping iteration. Our approach is based on similar estimates obtained in the finite element setting presented in the classical works of Douglas and Dupont [23] and Wheeler [81]. However, as is seen from (1) our PDE is degenerate for $x = 1$ which causes several difficulties. We overcome them by introducing a weighted L^2 space in which the solution is sought. We also utilize the extrapolation of coefficients in the way as was done in [45] to obtain a linear method. Galerkin finite element method has also been applied to parabolic equations with nonlocal terms in [38, 8]. A thorough survey of finite element method for parabolic equations can be found in [75]. On the other hand, Galerkin spectral methods has recently been applied to nonlinear parabolic problems in [44]. A different approach based on operator approximation and multivariate polynomial approximation has been taken in [1]. The reader can find a state-of-the-art surveys of all variants of spectral methods in [9, 71].

The paper is structured as follows. In the next section we present a derivation of our main model (1) in the climatological setting. In Section 3 we deal with semi-discrete scheme where we discretize the spatial variable leaving continuous dependence on time. The method attains an optimal spectral accuracy. The convergence proofs are given. Further, Section 4 concerns fully discrete method where a two-step weighted scheme with extrapolated coefficients is constructed and analysed with respect convergence. Thanks to the extrapolation, our method is linear despite the fact that the original problem may be highly nonlinear due to the diffusivity. In Section 5 we provide implementation guidelines, solutions that improve calculation performance, and simulations that verify previously proved estimates. We end the paper with a conclusion with some prospects on the future work.

In what follows the generic letter C will be used frequently to denote any positive constant that can depend on the solution and its derivatives but not on discretisation parameters. Moreover, as in the usual practice the value of C can change even in the same chain of inequalities. This will not cause any confusion or lack of rigour.

2 Background from climate dynamics

In order to set the stage for our subsequent reasoning we review the derivation of the main equation in the setting of climate dynamics. Some more elaborate exposition can be found in [27, 62].

We consider a simple conservation of energy written in terms of the zonally and vertically averaged temperature that is symmetric with respect to the equator. Let $T = T(x, t)$ be the mean temperature at time t and latitude θ where $x = \sin \theta$. We prefer to use x instead of θ since then, the spherical Laplacian simplifies substantially. The basic model is the following

$$cT_t = R_i - R_o + H, \quad (3)$$

where c is the heat capacity of Earth, R_i is the incoming solar radiation that reaches the surface (insolation), R_o is the outgoing infrared radiation, and H represents the horizontal transport.

We can further parametrize these various constituents. As the amount of heat Q reaches Earth its fraction α , called albedo, is reflected by the surface. Since, for example, snow ($\alpha = 0.80$) reflects much more light than ocean ($\alpha = 0.06$), we have to distinguish between different types of surface and its albedo. This leads to the so-called ice-albedo feedback that is one of the most important mechanisms regulating the climate. Since ice has a small albedo it causes more radiation to be reflected lowering the surface temperature. This, in turn, produces favourable conditions for formation of ice caps. This phenomenon can be parametrized by letting α to depend on x and T . In the literature one can find many of these functional relations. For example, Budyko proposed that the albedo has two values: one for ice and one for ice-free surface. The boundary between these, called the ice line, depends on the temperature

$$\alpha(x, t, T) = \begin{cases} \alpha_1, & T(x, t) \leq T_i, \\ \alpha_2, & T(x, t) > T_i, \end{cases} \quad (4)$$

where T_i is usually taken as -10°C . That is, ice starts to form when the mean temperature is below a threshold. This parametrization leads to a free-boundary problem since one has to determine the ice line position $x_0(t)$ satisfying $T(x_0(t), t) = T_i$. This approach has been analysed for example in [17, 48]. Other forms of albedo has also been proposed. One of the most common ones assume continuous dependence on both latitude and the temperature [29]. For example, Sellers suggested a piecewise linear relationship

$$\alpha(T) = \begin{cases} \alpha_1, & T \leq T_1, \\ \alpha_1 + (\alpha_2 - \alpha_1) \frac{T - T_1}{T_2 - T_1}, & T_1 < T \leq T_2, \\ \alpha_2, & T > T_2, \end{cases} \quad (5)$$

for some choices of $T_{1,2}$. In general, albedo is frequently represented as a bounded, monotone, increasing function of the temperature and, possibly, a low order polynomial in space [37, 5, 26, 62]. We will make such an assumption in the sequel. Moreover, as was suggested in [5] (but also see [64]), the present albedo of the ice-covered ground is determined not only by the actual temperature, but rather by its past values. Whence, we take α to be a function of the nonlocal (memory) operator acting on T , that is

$$R_i = QS(x, t)(1 - \alpha(x, T, JT)), \quad (6)$$

where $S = S(x, t)$ is the distribution of insolation over latitude which takes into account an uneven illumination of the spherical Earth. To a good approximation, one can take $S(x) \approx S_0 + S_1 L_2(x)$, where L_2 is the second Legendre polynomial [55].

Further, the absorbed heat is isotropically reradiated to space. This can be parametrized by the Stefan-Boltzmann law (as was done by Sellers)

$$R_o = \sigma T^4, \quad (7)$$

or its linearization $R_o = A + BT$ (as was done by Budyko). Since the change in the temperature is relatively small, this simplification is usually justified.

Finally, we have the horizontal transport term that arises due to uneven temperature distribution along the latitude: heat moves from equator to polar regions. On the level of complexity that we want to achieve we assume that the transport can be modelled by a diffusion term [52]

$$H = \nabla \cdot (d(u)\nabla T) = (d(u)(1 - x^2)T_x)_x. \quad (8)$$

Other approach, by Budyko, is based on using a relaxation term $\propto (T - \bar{T})$ where \bar{T} is the global mean temperature. The boundary conditions are taken to model the vanishing energy flux on both the equator $x = 0$ and poles $x = 1$, that is we impose $-D(u)(1 - x^2)T_x = 0$ there. As was found in [51, 52] linear diffusion, i.e. $D(u) = \text{const.}$, leads to an accurate and robust model and thus, is an important case to consider. However, as was suggested in [73] and further verified in [42], having the diffusivity being a function of the gradient has significant effect on stability of polar ice caps. This parametrization leads to the p-Laplacian operator which, in this case, was analysed in [16]. Putting all obtained terms and renaming the source term we arrive at (1).

We note that the heat capacity c is assumed to be constant, however, in [67] it was suggested that it may also be a function of the past values of the temperature and latitude. Investigating a model of this type along with gradient dependent diffusivity will be the subject of our future work.

3 Spectral discretization with respect to space

3.1 Definitions and assumptions

We begin with some preparations. By $L^2(0, 1)$ we denote the usual Hilbert space of square-integrable functions with a norm $\|\cdot\|$. Similarly, $H^m(0, 1)$ where $m \geq 1$ is the Sobolev space of m -th weakly differentiable functions with the norm denoted by $\|\cdot\|_m$. As for the scalar product we will only use the L^2 one and write (\cdot, \cdot) . We also introduce an intermediate space where the solution to (1) lives

$$V = \left\{ v \in H^1(0, 1) : \sqrt{1 - x^2} v_x \in L^2(0, 1) \right\}, \quad (9)$$

with the norm

$$\|v\|_V = \int_0^1 (1 - x^2) v_x^2 dx + \int_0^1 v^2 dx. \quad (10)$$

Due to degeneracy of the equation (1) at $x = 1$, the above weighted L^2 space is a natural choice [77]. Also, because of that reason the corresponding quadratic form needed for a definition of a weak solution is not coercive (it is only weakly coercive). One of the standard ways of dealing with that problem is to introduce a transformation

$$u(x, t) = e^{-t} T(x, t), \quad (11)$$

which leads to

$$\begin{cases} u_t + u = (D(u)(1 - x^2)u_x)_x + f(x, t, u, Ju), & x \in (0, 1), \quad t \in (0, t_0), \\ u_x(0, t) = 0, \quad u_x(1, t) < \infty, \\ u(x, s) = \psi(x, s), \quad -\tau \leq s \leq 0, \end{cases} \quad (12)$$

where $f(x, t, u, Ju) = e^{-t} g(x, t, e^t u, J(e^t u))$ and $\psi(x, s) = e^{-t} T_0(x, s)$. Notice that we should have written $D(t, u) = d(e^t u)$, i.e. indicate the explicit dependence on time. However, since $t \in [0, t_0]$ we have e^t bounded. Therefore, omitting it from the diffusivity will not produce any quantitative effects in the proofs below. We thus commit this slight abuse of notation and abstain from writing explicit

time dependence. The reader will see every reasoning below can be repeated for time dependent case with essentially no changes.

Now, by multiplying the above by $v \in V$ and integrating by parts from $x = 0$ to $x = 1$ we obtain a weak formulation which is the basis for the Galerkin method

$$\begin{cases} (u_t, v) + a(D(u); u, v) = (f(t, u, Ju), v), & v \in V, \\ u(s) = \psi(s), & -\tau \leq s \leq 0, \end{cases} \quad (13)$$

where the quadratic form a linear in the second and third argument is defined by

$$a(D(w); u, v) = \int_0^1 D(w)(1 - x^2)u_x v_x dx + \int_0^1 uv dx = (D(u)(1 - x^2)u_x, v_x) + (u, v). \quad (14)$$

We will also write $a(u, v) := a(1; u, v)$ which implies that $a(u, u) = \|u\|_V^2$. Moreover, from now on if it not posses any threat to unambiguity we will suppress writing the independent variables.

Concerning the assumptions imposed on various parameters we make the natural choices that are also required for existence and uniqueness (see [16, 67, 33]). Specifically, we assume that the diffusivity $D = D(u)$ and the source $f = f(x, t, u, w)$ are smooth with

$$0 < D_- \leq D(u) \leq D_+ < \infty, \quad |D_u| + |f_u| + |f_w| \leq C. \quad (15)$$

Moreover, we take the kernel of the nonlocal operator (2) to have a minimal regularity for well-posedness

$$K \in L^1(0, t_0). \quad (16)$$

In several places we will further assume that the solution of (12) is sufficiently smooth which, in turn, requires more regularity on D and f . We also would like to note that considering a discontinuous source case is one of the subjects of our future work.

3.2 Numerical scheme

In the spatial discretization we use the Galerkin scheme for which the test and trial functions (see [9]) belong to the following finite-dimensional space

$$V_N = \{v \in \mathbb{P}_N(0, 1) : v_x(0) = 0, v_x(1) < \infty\}, \quad (17)$$

where \mathbb{P}_N is the polynomial space of degree N . As for the orthonormal basis $\{\phi_i\}_{i=0}^N$ for V_N we choose

$$\phi_i = \sqrt{4n+1}L_{2i}(x), \quad i = 0, 1, 2, \dots, \quad (18)$$

where L_{2i} is the Legendre polynomial of degree $2i$. We obviously have $(\phi_i, \phi_j) = \delta_{ij}$. Moreover, this choice is particularly convenient for linear diffusion, i.e. $D(u) = \text{const.}$, because it constitutes the eigenbasis for the second order operator

$$L\phi_i := -((1 - x^2)(\phi_{i,x}))_x = \lambda_i \phi_i, \quad \lambda_i = 2i(2i + 1). \quad (19)$$

This automatically diagonalizes the stiffness matrix and facilitates computations in the important linear case or makes the matrix sparse for weakly nonlinear diffusion.

By weighting (13) with respect to V_N we formulate the Legendre-Galerkin numerical scheme. We thus look for $u_N(t) \in V_N$ that for all $t \in [0, t_0]$ satisfies

$$\begin{cases} (u_{N,t}, v) + a(D(u_N); u_N, v) = (f(t, u_N, Ju_N), v), & v \in V_N, \\ u_N(s) = \psi_N(s), & -\tau \leq s \leq 0, \end{cases} \quad (20)$$

where ψ_N is the appropriate approximation to the initial condition. Henceforth, we will use the orthogonal L^2 Legendre projection

$$\psi_N(s) = P_N\psi(s) := \sum_{i=0}^N (\psi(s), \phi_i) \phi_i, \quad -\tau \leq s \leq 0, \quad (21)$$

which has the following spectral accuracy (for a detailed discussion see [9], formulas (5.4.12) and (5.4.17))

$$\begin{aligned} \|u - P_N u\| &\leq C N^{-m} \|u\|_m, \quad \|u - P_N u\|_l \leq C N^{2l-1/2-m} \|u\|_m, \\ \|u - P_N u\|_\infty &\leq C N^{\frac{1}{2}-m} V(u_x^{(m)}), \end{aligned} \quad (22)$$

where $V(\cdot)$ denoted the total variation and $l \geq 1$. The error of the approximation with P_N in V -norm is somewhat better than in the Sobolev space.

Lemma 1. *Let $u(t) \in H^{2m}(0, 1)$ for $m \geq 1$ and each $t \in [0, t_0]$ with u and u_t bounded. Then, for sufficiently large N we have*

$$\|u - P_N u\|_V \leq C N^{1-2m} \|L^m u\| \leq C N^{1-2m} \|u\|_{2m}, \quad (23)$$

where L is defined in (19).

Proof. We start by writing

$$((1-x^2)(u - P_N u)_x, (u - P_N u)_x) = \int_0^1 (u - P_N u) L(u - P_N u) dx, \quad (24)$$

where we have integrated by parts. Since

$$u - P_N u = \sum_{i=N+1}^{\infty} (u, \phi_i) \phi_i, \quad (25)$$

we obtain

$$((1-x^2)(u - P_N u)_x, (u - P_N u)_x) = \sum_{i,j=N+1}^{\infty} (u, \phi_i)(u, \phi_j) \int_0^1 \phi_i L \phi_j dx. \quad (26)$$

Moreover, since ϕ_i is the eigenfunction of L (see (19)) we have

$$((1-x^2)(u - P_N u)_x, (u - P_N u)_x) = \sum_{i=N+1}^{\infty} \lambda_i |(u, \phi_i)|^2. \quad (27)$$

However, we can also write $\phi_i = \lambda_i^{-1} L \phi_i$ which after iteration implies that

$$((1-x^2)(u - P_N u)_x, (u - P_N u)_x) = \sum_{i=N+1}^{\infty} \lambda_i^{1-2m} |(u, L^m \phi_i)|^2 \leq \lambda_{N+1}^{1-2m} \|L^m u\|^2, \quad (28)$$

where the last inequality follows from Plancherel's identity. Further, since $\lambda_{N+1} = (2N+2)(2N+3)$ we can write

$$((1-x^2)(u - P_N u)_x, (u - P_N u)_x) \leq C N^{2-4m} \|L^m u\|^2. \quad (29)$$

Now, by the L^2 error estimates for P_N given in (22) we have

$$((1-x^2)(u - P_N u)_x, (u - P_N u)_x) + (u - P_N u, u - P_N u) \leq C (N^{2-4m} \|L^m u\|^2 + N^{-4m} \|u\|_{2m}^2), \quad (30)$$

which for sufficiently large N implies the sought error estimate in the V -norm. \square

We note that the above is not the only optimal choice of a projection that we can use. In fact, for the main equation (20) it is much more convenient to use the following elliptic (or Ritz) orthogonal projection

$$a(D(u); R_N u - u, v) = 0, \quad v \in V_N, \quad (31)$$

which utility in obtaining an optimal order of convergence was discovered in the early days of mathematical finite element analysis (see the seminal paper by Wheeler [81]).

Before we proceed the convergence result for (20) we state several auxiliary lemmas concerning Ritz projection (31). First, we show that it has the optimal order of approximation both in V and in $L^2(0, 1)$.

Lemma 2. *Let $u(t) \in H^{2m}(0, 1)$ for $m \geq 1$ and each $t \in [0, t_0]$ with u and u_t bounded. Then, for sufficiently large N we have the following estimate in V and L^2*

$$\|u - R_N u\| + N^{-1} \|u - R_N u\|_V \leq C N^{-2m} \|u\|_{2m}. \quad (32)$$

Moreover, if additionally $u_t \in H^{2m}(0, 1)$ then the time derivatives of the errors satisfy

$$\|(u - R_N u)_t\| + N^{-1} \|(u - R_N u)_t\|_V \leq C N^{-2m} (\|u\|_{2m} + \|u_t\|_{2m}). \quad (33)$$

Proof. By (14) and since $R_N u \in V_N$ we have

$$D_- \|u - R_N u\|_V^2 \leq a(D(u); u - R_N u, u - R_N u) = a(D(u); u - R_N u, u - v) + a(D(u); u - R_N u, v - R_N u), \quad (34)$$

where $v \in V_N$. By orthogonality of the Ritz projection (31) the last term above vanishes leaving

$$D_- \|u - R_N u\|_V^2 \leq D_+ a(u - R_N u, u - v), \quad v \in V_N. \quad (35)$$

By choosing $v = P_N u$ and using Cauchy-Schwarz inequality we immediately have

$$\|u - R_N u\|_V^2 \leq \frac{D_+}{D_-} \|u - R_N u\|_V \|u - P_N u\|_V, \quad (36)$$

which by Lemma 1 leads to

$$\|u - R_N u\|_V \leq \frac{D_+}{D_-} \|u - P_N u\|_V \leq C N^{1-m} \|u\|_m, \quad (37)$$

which is the first assertion.

In order to show the L^2 estimate on the error we follow the duality argument (see [75]). For a fixed $u \in H^{2m}(0, 1)$ let w be the solution of

$$a(D(u); w, v) = (u - R_N u, v), \quad v \in V. \quad (38)$$

By putting $v = w$ we immediately obtain the stability estimate $\|w\|_V \leq C \|u - R_N u\|$. Using the definition of a as in (14) and reintegrating by parts we can obtain

$$\|Lw\| \leq C \|u - R_N u\| + \|w\| \leq C \|u - R_N u\| + \|w\|_V \leq C \|u - R_N u\|, \quad (39)$$

where the assumption of bounded D has been used in the first inequality while the stability estimate in the last. Now, by choosing $v = u - R_N u$ in (38) and using the definition of the Ritz projection (31) we have

$$\begin{aligned} \|u - R_N u\|^2 &= (u - R_N u, u - R_N u) = a(D(u); w, u - R_N u) \\ &= a(D(u); w - P_N w, u - R_N u) + a(D(u); P_N w, u - R_N u) \\ &= a(D(u); w - P_N w, u - R_N u). \end{aligned} \quad (40)$$

Further, we can use Cauchy-Schwarz inequality along with (37) and (23) to infer that

$$\|u - R_N u\|^2 \leq D_+ \|w - P_N w\|_V \|u - R_N u\|_V \leq C N^{1-2} \|Lw\| N^{1-2m} \|u\|_{2m}. \quad (41)$$

The proof of (32) is finished after utilizing (39).

The reasoning used in showing the time differentiated version (33) is similar and based on a derivative of the Ritz projection definition (31)

$$a(D(u); (R_N u - u)_t, v) + a(D(u)_t; R_N u - u, v) = 0, \quad v \in V_N. \quad (42)$$

From here it follows that

$$\begin{aligned} D_- \|(R_N u - u)_t\|_V^2 &\leq a(D(u); (R_N u - u)_t, (R_N u - u)_t) \\ &= a(D(u); (R_N u)_t - v, (R_N u - u)_t) + a(D(u); v - u_t, (R_N u - u)_t) \\ &= a(D(u)_t; v - (R_N u)_t, R_N u - u) + a(D(u); v - u_t, (R_N u - u)_t). \end{aligned} \quad (43)$$

Now, Cauchy-Schwarz inequality yields

$$D_- \|(R_N u - u)_t\|_V^2 \leq C (\|v - (R_N u)_t\|_V \|R_N u - u\|_V + \|v - u_t\|_V \|(R_N u - u)_t\|_V). \quad (44)$$

We can make the norms of differences sufficiently small by orthogonal approximation, i.e. by choosing $v = P_N u_t$. Whence,

$$D_- \|(R_N u - u)_t\|_V^2 \leq C (\|(P_N u - R_N u)_t\|_V \|R_N u - u\|_V + \|(P_N u - u)_t\|_V \|(R_N u - u)_t\|_V), \quad (45)$$

and by another estimate

$$\|(P_N u - R_N u)_t\|_V \leq \|(P_N u - u)_t\|_V + \|(u - R_N u)_t\|_V, \quad (46)$$

we can write

$$\begin{aligned} D_- \|(R_N u - u)_t\|_V^2 &\leq C (\|(P_N u - u)_t\|_V \|R_N u - u\|_V + \|(u - R_N u)_t\|_V \|R_N u - u\|_V \\ &\quad + \|(P_N u - u)_t\|_V \|(u - R_N u)_t\|_V). \end{aligned} \quad (47)$$

We can now use the ϵ -Cauchy inequality, that is

$$ab \leq \frac{\epsilon}{2} a^2 + \frac{1}{2\epsilon} b^2, \quad a, b \in \mathbb{R}, \quad \epsilon > 0, \quad (48)$$

to transform our estimate to

$$D_- \|(R_N u - u)_t\|_V^2 \leq \frac{D_-}{2} \|(R_N u - u)_t\|_V^2 + C (\|(P_N u - u)_t\|_V + \|u - R_N u\|_V)^2, \quad (49)$$

that is

$$\|(R_N u - u)_t\|_V \leq C (\|(P_N u - u)_t\|_V + \|u - R_N u\|_V). \quad (50)$$

Hence, the V -norm part of (33) follows from (23) and (32).

The L^2 estimate again follows from the duality argument. Let w be as before in (38) but $(u - R_N u)_t$ on the right-hand side. Reasoning similarly as before we have with $v \in V$

$$\begin{aligned} \|(u - R_N u)_t\|^2 &= a(D(u); w, (u - R_N u)_t) \\ &= a(D(u); w - v, (u - R_N u)_t) + a(D(u); v, (u - R_N u)_t) \\ &= a(D(u); w - v, (u - R_N u)_t) - a(D(u)_t; v, u - R_N u) \\ &= a(D(u); w - v, (u - R_N u)_t) + a(D(u)_t; w - v, u - R_N u) - a(D(u)_t; w, u - R_N u). \end{aligned} \quad (51)$$

where in the third equality we have moved the derivative according to (42) while in the last we have introduced w . Thanks to that, with $v = P_N w$ we can bound the above by previously obtained estimates in the V -norm

$$\|(u - R_N u)_t\|^2 = C(\|w - P_N w\|_V (\|(u - R_N u)_t\|_V + \|u - R_N u\|_V) + |a(w - P_N w, u - R_N u)|). \quad (52)$$

The first two terms can be tackled exactly in the same way as above, and the third term can be integrated by parts to obtain

$$\begin{aligned} |a(w - P_N w, u - R_N u)| &\leq \int_0^1 |Lw| |u - R_N u| dx \leq \|Lw\| \|u - R_N u\| \\ &\leq C \|(u - R_N u)_t\| \|u - R_N u\|, \end{aligned} \quad (53)$$

by stability estimate for elliptic equation (39). Finally, combining the two above estimates with (32) yields (42) and finishes the proof. \square

As we have seen, the elliptic projection has the same order of accuracy as the standard projection P_N . Note also that the error in the V -norm is bounded by N^{1-2m} for sufficiently regular functions u . This norm involves the first derivative and is similar to the standard H^1 norm with $\|u\|_V \leq \|u\|_1$. This can be compared with the classical result concerning approximation in H^1 which states that in that case the error is proportional to $N^{3/2-2m}$ which is larger than the former estimate. This again shows that choosing V as the trial space is very natural and optimal.

The Ritz projection is also bounded in the maximum norm which is shown below.

Lemma 3. *Let R_N be defined as in (31) and $u \in H^4(0, 1)$. Then, for sufficiently large N we have*

$$\|(R_N u)_x\|_\infty \leq \|u_x\|_\infty. \quad (54)$$

Proof. We will use the following polynomial inverse inequalities, one for differentiation (Markov inequality, [76], p. 218), and the other for summability (see [9], formulas (5.4.3) and (5.4.5))

$$\|v_x\|_\infty \leq CN^2 \|v\|_\infty \leq CN^3 \|v\|, \quad v \in \mathbb{P}_N. \quad (55)$$

Now, we can write

$$\|(R_N u)_x\|_\infty \leq \|(R_N u - u)_x\|_\infty + \|u_x\|_\infty, \quad (56)$$

and use the above inverse inequality and the error estimate (32)

$$\|(R_N u)_x\|_\infty \leq CN^3 \|R_N u - u\| + \|u_x\|_\infty \leq CN^{3-4} \|u\|_4 + \|u_x\|_\infty, \quad (57)$$

from which the conclusion follows for sufficiently large N . \square

The last auxiliary result is the classical Grönwall-Bellman's lemma that we state without the proof (which can be found in [43]).

Lemma 4 (Grönwall-Bellman). *Let $F(t)$ and $y(t)$ be continuous and nonnegative functions. Then*

$$y(t) \leq F(t) + C \int_0^t y(s) ds, \quad (58)$$

implies

$$y(t) \leq F(t) e^{Ct}. \quad (59)$$

We are ready to prove the main results of this section concerning semi-discrete numerical scheme. First, we show that the method is stable in time.

Theorem 1 (Stability). Assume that $f = f(x, t, u, w)$ is bounded with respect to u , and w , that is

$$\|f(x, t, u, w)\|_\infty \leq g(x, t). \quad (60)$$

Then, if u_N is the solution of (20), we have

$$\|u_N(t)\| \leq e^{-D_-(\lambda_1-1)t} \|\psi_N(0)\| + \int_0^1 e^{-D_-(\lambda_1-1)(t-s)} \|g(s)\| ds, \quad (61)$$

where D_- is given in (15) while λ_1 is defined in (19).

Proof. The proof is standard: in (20) choose $v = u_N$, use Cauchy-Schwarz inequality, and the boundedness assumption to obtain

$$\frac{1}{2} \frac{d}{dt} \|u_N(t)\|^2 + a(D(u_N); u_N, u_N) \leq \|g(t)\| \|u_N(t)\|. \quad (62)$$

Now, since $a(D(u_N); u_N, u_N) \geq D_- a(u_N, u_N)$ (see (14) and (15)) we can write

$$\|u_N(t)\| \frac{d}{dt} \|u_N(t)\| + D_- a(u_N, u_N) \leq \|g(t)\| \|u_N(t)\|, \quad (63)$$

which after division by $\|u_N(t)\|$ leads to

$$\frac{d}{dt} \|u_N(t)\| + D_- \frac{a(u_N, u_N)}{\|u_N(t)\|^2} \|u_N(t)\| \leq \|g(t)\|. \quad (64)$$

The left-hand side is bounded from below by the infimum over the whole space V , hence

$$\frac{d}{dt} \|u_N(t)\| + D_- \inf_{v \in V} \frac{a(v, v)}{\|v\|^2} \|u_N(t)\| \leq \|g(t)\|. \quad (65)$$

According to standard theory of elliptic PDEs the infimum can be interpreted as

$$\inf_{v \in V} \frac{a(v, v)}{\|v\|^2} = \lambda_1 - 1, \quad (66)$$

which is the smallest eigenvalue of the problem $a(u, v) = \lambda(u, v)$ with $v \in V$ and λ_1 is given in (19). Finally, multiplying the inequality by the factor $e^{D_-(\lambda_1-1)t}$ and integrating yields the sought result. \square

Again, we can see the close relationship between the linear diffusion generated by operator L and the fully nonlinear case. We can now proceed to the convergence proof.

Theorem 2 (Convergence). Let $u(t)$ and $u_N(t)$ be solutions of (13) and (20), respectively belonging to $H^{2m}(0, 1)$ with $m \geq 4$ for each $t \in [0, t_0]$. Moreover, assume that u_x and u_t are bounded. Then, for sufficiently large N and for each $t \in [0, t_0]$ we have

$$\begin{aligned} \|u(t) - u_N(t)\| &\leq \|R_N(t) - u(t)\| \\ &+ C \left(\|P_N \psi(0) - \psi(0)\| + \|R_N \psi(0) - \psi(0)\| + \int_0^t (\|(R_N - u)_t(z)\| + \|(R_N - u)(z)\|) dz \right), \end{aligned} \quad (67)$$

in particular

$$\|u(t) - u_N(t)\| \leq CN^{-2m}, \quad (68)$$

where the constant C depends on u , u_x , u_t , D , f , and K .

Proof. We start by decomposing the error

$$u - u_n = u - R_N u + R_N u - u_N =: r_N + e_N. \quad (69)$$

Therefore, since we have already proved the estimates on r_N in Lemma 2 we have to focus only on e_N . To this end, we will write the error equation. For $v \in V_N$ we have

$$\begin{aligned} (e_{N,t}, v) + a(D(u_N); e_N, v) &= (R_N u_t, v) + a(D(u_N); R_N u, v) - (u_{N,t}, v) + a(D(u_N); u_N, v) \\ &= (R_N u_t, v) + a(D(u_N); R_N u, v) - (f(t, u_N, Ju_N), v), \end{aligned} \quad (70)$$

where we have used (20). Further, by using the main equation (13) and the definition of the Ritz projection (31) we can obtain

$$\begin{aligned} (e_{N,t}, v) + a(D(u_N); e_N, v) &= (R_N u_t, v) + a(D(u); R_N u, v) + a(D(u_N) - D(u); R_N u, v) - (f(t, u_N, Ju_N), v) \\ &= (R_N u_t, v) + a(D(u); u, v) + a(D(u_N) - D(u); R_N u, v) - (f(t, u_N, Ju_N), v) \\ &= ((R_N u - u)_t, v) + a(D(u_N) - D(u); R_N u, v) - (f(t, u_N, Ju_N) - f(t, u, Ju), v). \end{aligned} \quad (71)$$

Therefore, by taking $v = e_N \in V_N$ we are lead to the estimate

$$\begin{aligned} \frac{1}{2} \frac{d}{dt} \|e_N\|^2 + D_- \|e_N\|_V^2 &\leq |(r_{N,t}, e_N)| + |a(D(u_N) - D(u); R_N u, e_N)| \\ &\quad + |(f(t, u_N, Ju_N) - f(t, u, Ju), e_N)| =: \rho_1 + \rho_2 + \rho_3. \end{aligned} \quad (72)$$

And from here we are left to estimate the three remainders ρ_i . The first one comes from (33), while for the second we use (15) and obtain

$$\rho_2 \leq C \int_0^1 |u_N - u|(1 - x^2) |(R_N u)_x| |e_{N,x}| dx. \quad (73)$$

Now, the gradient of the Ritz projection is bounded according to Lemma 3 and hence

$$\rho_2 \leq C \int_0^1 |u_N - u|(1 - x^2) |e_{N,x}| dx \leq C \|u_N - u\| \|e_N\|_V \leq C (\|r_N\| \|e_N\|_V + \|e_N\| \|e_N\|_V). \quad (74)$$

The third remainder can be bounded using (15)

$$\rho_3 \leq C (\|u - u_N\| + \|Ju - Ju_N\|) \|e_N\| \leq C (\|r_N\| + \|e_N\| + \|J(u - u_N)\|) \|e_N\|. \quad (75)$$

Now, the nonlocal operator Ju is defined by (2) and hence

$$\begin{aligned} \|J(u - u_N)(t)\| &\leq \int_0^\tau K(s) \|u(t - s) - u_N(t - s)\| ds \\ &\leq \int_0^\tau K(s) \|r_N(t - s)\| ds + \int_0^\tau K(s) \|e_N(t - s)\| ds \\ &\leq \int_0^t K(t - s) \|r_N(s)\| ds + \int_0^t K(t - s) \|e_N(s)\| ds, \end{aligned} \quad (76)$$

where in the last inequality we have changed the integration variable $s \mapsto t - s$ and used the fact that the integral of a positive function over $[0, t]$ is larger than over $[t - \tau, t]$. Finally, we can combine all the estimates on ρ_i and use ϵ -Cauchy inequality where necessary to extract $\|e_N\|_V^2$ and bound products of norms in terms of sum of their squares. In the effect, we arrive at

$$\begin{aligned} \frac{1}{2} \frac{d}{dt} \|e_N\|^2 + D_- \|e_N\|_V^2 &\leq \frac{D_-}{2} \|e_N\|_V^2 \\ &\quad + C \left(\|r_{N,t}\|^2 + \|e_N\|^2 + \int_0^t K(t - s) \|r_N(s)\|^2 ds + \int_0^t K(t - s) \|e_N(s)\|^2 ds \right), \end{aligned} \quad (77)$$

whence

$$\frac{d}{dt} \|e_N\|^2 \leq C \left(\|r_{N,t}\|^2 + \int_0^t K(t-s) \|r_N(s)\|^2 ds + \|e_N\|^2 + \int_0^t K(t-s) \|e_N(s)\|^2 ds \right). \quad (78)$$

By integrating the above we obtain

$$\begin{aligned} \|e_N(t)\|^2 &\leq \|e_N(0)\|^2 + C \left(\int_0^t \|r_{N,t}(z)\|^2 dz + \int_0^t \left(\int_0^{t-s} K(s) ds \right) \|r_N(z)\|^2 dz \right. \\ &\quad \left. + \int_0^t \left[1 + \left(\int_0^{t-z} K(s) ds \right) \right] \|e_N(z)\|^2 dz \right). \end{aligned} \quad (79)$$

Since K is integrable, its integral is continuous, hence bounded and

$$\|e_N(t)\|^2 \leq \|e_N(0)\|^2 + C \left(\int_0^t (\|r_{N,t}(z)\|^2 + \|r_N(z)\|^2) dz + \int_0^t \|e_N(z)\|^2 dz \right), \quad (80)$$

and we can invoke Grönwall-Bellman's Lemma (Lemma 4) to arrive at

$$\begin{aligned} \|e_N(t)\|^2 &\leq \left(\|e_N(0)\|^2 + C \int_0^t (\|r_{N,t}(z)\|^2 + \|r_N(z)\|^2) dz \right) e^{Ct} \\ &\leq C \left(\|e_N(0)\|^2 + \int_0^t (\|r_{N,t}(z)\|^2 + \|r_N(z)\|^2) dz \right), \end{aligned} \quad (81)$$

since $t \in [0, t_0]$. This, Lemma 2 and the fact that $u - u_N = r_n + e_N$ implies the assertion and completes the proof. \square

4 Weighted linear time-stepping scheme

We would like to fully discretize (20) to obtain a time-stepping numerical scheme. However, in order to reduce the computational cost, we would like to obtain a linear method. To this end, we will use extrapolation of the nonlinear coefficients (see [75, 45]) along with a θ -weighed scheme.

As a preparation we introduce the temporal grid on $[0, t_0]$ with a step h is defined as

$$t_n = nh, \quad h = n \frac{t_0}{N_0}, \quad (82)$$

where N_0 is the number of subintervals. Further, if U^n is a grid function, that is a function defined on t_n with $n = 0, \dots, N_0$ that can be thought as a piecewise constant function on $[0, t_0]$, we define the usual finite difference

$$\delta U^n = \frac{U^{n+1} - U^n}{h}. \quad (83)$$

Further, we have to discretize the nonlocal operator (2) and in general the discretization can be written for $\tau = hM$

$$J_h U^n = \sum_{i=0}^M w_i(K) U^{n-i} + \rho_0(h), \quad (84)$$

where $\rho(h)$ is the local consistency error, and $w_i(K)$ are weights. In particular, we can choose the rectangle rule to have for $0 \leq i < M$

$$w_i(K) = \begin{cases} \int_{t_i}^{t_{i+1}} K(s) ds, & 0 \leq i < M, \\ 0, & i = M, \end{cases} \quad (85)$$

or trapezoid rule

$$w_i(K) = \begin{cases} \int_0^h K(s) \left(1 - \frac{s}{h}\right) ds, & i = 0, \\ \int_{t_i}^{t_{i+1}} K(s) \left(1 - \frac{s - t_i}{h}\right) ds + \int_{t_{i-1}}^{t_i} K(s) \frac{s - t_{i-1}}{h} ds, & 1 \leq i < M, \\ \int_{\tau-h}^{\tau} K(s) \frac{s - \tau + h}{h} ds, & i = M. \end{cases} \quad (86)$$

Provided sufficient smoothness, the orders of the above quadratures are: first for the rectangle, and second for the trapezoid. Note that we have used the so-called product integration rule, that is we have discretized the unknown function U leaving the exact integral of the kernel. This procedure guarantees maximal order of convergence for sufficiently smooth U (see [43]).

In order to state the method we define the θ -averaged value

$$\widehat{U}^{n-\theta} := (1 - \theta)U^{n-1} + \theta U^n, \quad 0 \leq \theta \leq 1, \quad (87)$$

and its extrapolation through the past two time steps

$$\overline{U}^{n-\theta} := (1 + \theta)U^{n-1} - \theta U^{n-2}, \quad 0 \leq \theta \leq 1. \quad (88)$$

It can be easily seen by Taylor series expansion that

$$|\widehat{U}^{n-\theta} - \overline{U}^{n-\theta}| = O(h^2), \quad h \rightarrow 0^+. \quad (89)$$

Now, we fix $N > 0$ as the number of terms in the Galerkin semi-discrete solution of (20) and set U^n to be the numerical approximation to $u_N(t_n)$. Note that we will omit writing subindex N in our fully discrete approximation. We then propose the following scheme for solving (12)

$$(\delta U^n, v) + a(D(\overline{U}^{n-\theta}); \widehat{U}^{n-\theta}, v) = (f_h(\overline{U}^{n-\theta}), v), \quad v \in V_N, \quad (90)$$

where f_h is defined as

$$f_h(U^n) = f(x, t_n, U^n, J_h U^n), \quad (91)$$

which is a full discretization of the source nonlinearity. Note that since we are using extrapolation (88) in D and f we are required to solve only a linear system of equation in each time step. This technique of removing nonlinearity is a classical move developed in [45]. Due to a weighted nature of (90) we obtain the first order backward Euler method for $\theta = 1$ and second order Crank-Nicolson scheme for $\theta = 1/2$. Accordingly, with respect to requirements, one can choose either the rectangle or trapezoid quadrature in (84).

To complete the numerical scheme we have to state the initialization procedure. Since the extrapolation produced a two-step method we have to carefully start the iteration for the order to be preserved. We use the predictor-corrector method. The predictor step is based on setting $U^0 = \psi_N(0)$ and solving for W in

$$(P) \quad h^{-1}(W - U^0, v) + a(D(U^0); U^{1-\theta}, v) = (f_h(U^0), v) \quad v \in V_N. \quad (92)$$

Then, we correct the value of W by

$$(C) \quad h^{-1}(U^1 - W, v) + a(D(W^{1-\theta}); U^{1-\theta}, v) = (f_h(W^{1-\theta}), v) \quad v \in V_N, \quad (93)$$

where $W^{1-\theta} = (1 - \theta)U^0 + \theta W$. This gives us two starting values U^0, U^1 that can be plugged into the time-stepping (90).

We now move to the convergence result.

Theorem 3 (Convergence of the full discrete scheme). *Let $u(t) \in H^{2m}(0, 1)$ for each $t \in [0, t_0]$ with $m \geq 1$. Further, assume that u_x , u_t , and u_{tt} are bounded. Then,*

$$\|u^n - U^n\| \leq C \left(N^{-2m} + \rho_0(h) \left(\theta - \frac{1}{2} \right) h + h^2 \right), \quad (94)$$

where the constant C depends on u , ψ and all their derivatives, and $\rho_0(h)$ is defined in (84).

Proof. Similarly as in the proof of the semi-discrete scheme we start by decomposing the error

$$u^n - U^n = u^n - R_N u^n + R_N u^n - U^n =: r^n + e^n, \quad (95)$$

where $u^n = u(t_n)$ and we keep our convention not to write N explicitly (since it is fixed). Then, we start writing the error equation with $v \in V_N$

$$\begin{aligned} (\delta e^n, v) + a(D(\bar{U}^{n-\theta}); \hat{e}^{n-\theta}, v) \\ = (\delta R_N u^n, v) + a(D(\bar{U}^{n-\theta}); R_N \hat{U}^{n-\theta}, v) - (\delta U^n, v) - a(D(\bar{U}^{n-\theta}); \hat{U}^{n-\theta}, v) \\ = (\delta R_N u^n, v) + a(D(\bar{U}^{n-\theta}); R_N \hat{U}^{n-\theta}, v) - (f_h(\bar{U}^{n-\theta}), v), \end{aligned} \quad (96)$$

where in the last equality we have used (90). Expanding further we have

$$\begin{aligned} (\delta e^n, v) + a(D(\bar{U}^{n-\theta}); e^{n-\theta}, v) \\ = (\delta R_N u^n, v) + a(D(\bar{U}^{n-\theta}) - D(u^{n-\theta}); R_N \hat{U}^{n-\theta}, v) \\ + a(D(u^{n-\theta}); R_N \hat{U}^{n-\theta} - R_N u^{n-\theta}, v) + a(D(u^{n-\theta}); R_N u^{n-\theta}, v) - (f_h(\bar{U}^{n-\theta}), v) \\ = (\delta R_N u^n - u_t^{n-\theta}, v) + a(D(\bar{U}^{n-\theta}) - D(u^{n-\theta}); R_N \hat{U}^{n-\theta}, v) \\ + a(D(u^{n-\theta}); R_N \hat{U}^{n-\theta} - R_N u^{n-\theta}, v) + (f(u^{n-\theta}) - f_h(\bar{U}^{n-\theta}), v) \end{aligned} \quad (97)$$

where this time we have used the main equation (13). In the above we would like to put $v = \hat{e}^{n-\theta}$ in order to derive estimates on the error. Before that, however, note that

$$(\delta e^n, \hat{e}^{n-\theta}) = \frac{1}{2} \delta \|e^n\|^2 + h \left(\theta - \frac{1}{2} \right) \|\delta e^n\|^2, \quad (98)$$

which can be shown by expanding the definitions of δe^n and $\hat{e}^{n-\theta}$. Note that we see that taking $\theta = 1/2$ kills the $O(h)$ term. Therefore, with the aforementioned choice of v , we can write

$$\frac{1}{2} \delta \|e^n\|^2 + h \left(\theta - \frac{1}{2} \right) \|\delta e^n\|^2 + D_- \|\hat{e}^n\|_V^2 \leq \rho_1 + \rho_2 + \rho_3 + \rho_4, \quad (99)$$

where the remainders ρ_i are understood from (97). We will now bound each of them.

We start with the difference in time derivatives

$$\|\delta R_N u^n - u_t^{n-\theta}\| \leq \|\delta r^n\| + \|\delta u^n - u_t^{n-\theta}\|. \quad (100)$$

Now, by Taylor expansion at $t = t_{n-\theta} = (n - \theta)h$ we obtain

$$\begin{aligned} \delta u^n - u_t^{n-\theta} &= h^{-1} (u^{n-\theta} + h\theta u_t^{n-\theta} - u^{n-\theta} + (1 - \theta)h u_t^{n-\theta} + \\ &\quad \frac{1}{2} h^2 \theta^2 u_{tt}^{n-\theta} - h^2 (1 - \theta)^2 u_{tt}^{n-\theta} + O(h^3)) - u_t^{n-\theta} \\ &= h \left(\theta - \frac{1}{2} \right) u_{tt}^{n-\theta} + O(h^2), \quad h \rightarrow 0^+. \end{aligned} \quad (101)$$

Whence, by Lemma 2 we have

$$\rho_1 \leq C \left(N^{-2m} + h \left(\theta - \frac{1}{2} \right) + h^2 \right) \|\hat{e}^{n-\theta}\|. \quad (102)$$

Next, the remainder associated with a can be bounded thanks to (15)

$$\rho_2 \leq C \|R_N \hat{u}^{n-\theta}\|_\infty \|\bar{U}^{n-\theta} - u^{n-\theta}\| \|\hat{e}^{n-\theta}\|_V, \quad (103)$$

and the difference between extrapolated and the value of the exact solution can be estimated as follows

$$\begin{aligned} \|\bar{U}^{n-\theta} - u^{n-\theta}\| &\leq \|\bar{U}^{n-\theta} - \bar{u}^{n-\theta}\| + \|\bar{u}^{n-\theta} - u^{n-\theta}\| \leq \|\bar{e}^{n-\theta}\| + \|\bar{r}^{n-\theta}\| + \|\bar{u}^{n-\theta} - u^{n-\theta}\| \\ &\leq C (\|e^{n-1}\| + \|e^{n-2}\| + N^{-2m} + h^2), \end{aligned} \quad (104)$$

since, by construction, $\bar{u}^{n-\theta}$ approximates $u^{n-\theta}$ to the second order. Next, we proceed to the third remainder to obtain

$$\rho_3 \leq C \|R_N \hat{u}^{n-\theta} - R_N u^{n-\theta}\|_V \|\hat{e}^{n-\theta}\|_V \leq D_- \|\hat{e}^{n-\theta}\|_V^2 + C \|R_N \hat{u}^{n-\theta} - R_N u^{n-\theta}\|_V^2, \quad (105)$$

where we have used the ϵ -Cauchy inequality to extract the V -norm of the error. But, exactly as above due to Taylor expansion at $t = t_{n-\theta} = (n - \theta)h$ we have for any function y of time

$$\|\hat{y}^{n-\theta} - y^{n-\theta}\| \leq \frac{1}{2} h \left(\theta - \frac{1}{2} \right) y_t^{n-\theta} + \frac{1}{2} h^2 (\theta^3 - (1 - \theta)^3) \hat{y}_{tt}^{n-\theta}. \quad (106)$$

In order to apply this estimate to the ρ_3 we have to show that the gradient of the second time derivative of Ritz projection is bounded in V . To this end, differentiate the definition (31) twice to obtain

$$a(D(u); R_N u - u, v) = -(D(u)_{tt}; r, v) - 2(D(u)_t; r_t, v) + (D(u); u_{tt}, v). \quad (107)$$

From here, with a choice $v = (R_N u)_{tt}$ we have

$$\|(R_N u)_{tt}\|_V \leq C (\|r\|_V + \|r_t\|_V + \|u_{tt}\|_V) \leq C \|u_{tt}\|_V, \quad (108)$$

for sufficiently large N by Lemma 2. Whence, according to Lemma 2 we finally obtain

$$\rho_3 \leq D_- \|\hat{e}^{n-\theta}\|_V^2 + C \left(h \left(\theta - \frac{1}{2} \right) + h^2 \right)^2. \quad (109)$$

The last remainder involves nonlocal operator. First, we estimate the difference by the regularity assumption on f

$$\|f(u^{n-\theta}) - f_h(\bar{U}^{n-\theta})\| = C \left(\|\bar{U}^{n-\theta} - u^{n-\theta}\| + \|J_h \bar{U}^{n-\theta} - J u^{n-\theta}\| \right). \quad (110)$$

Now, by (84) we have

$$\begin{aligned} \|J_h \bar{U}^{n-\theta} - J u^{n-\theta}\| &\leq C \rho_0(h) + \sum_{i=0}^M w_i(K) \|\bar{U}^{n-\theta-i} - u^{n-\theta-i}\| \\ &\leq C \rho_0(h) + \sum_{i=0}^M w_i(K) (\|\bar{r}^{n-\theta}\| + h^2) + \sum_{i=0}^M w_i(K) \|\bar{e}^{n-\theta-i}\| \\ &\leq C(\rho_0(h) + h^2 + N^{-2m}) + \sum_{i=0}^M w_i(K) \|\bar{e}^{n-\theta-i}\|, \end{aligned} \quad (111)$$

by integrability of the kernel K . Hence,

$$\rho_4 \leq C \left(\rho_0(h) + h^2 + N^{-2m} + \sum_{i=0}^M w_i(K) \|\bar{e}^{n-\theta-i}\| \right) \|\hat{e}^{n-\theta}\|. \quad (112)$$

Putting all estimates of ρ_i that we have obtained so far and defining

$$\rho(N, h) := \rho_0(h) + h^2 + N^{-2m}, \quad (113)$$

leads to

$$\frac{1}{2} \delta \|e^n\|^2 \leq C \left(\rho(N, h)^2 + \|e^{n-1}\|^2 + \|e^{n-2}\|^2 + \left(\sum_{i=0}^M w_i(K) \|\bar{e}^{n-\theta-i}\| \right)^2 \right), \quad (114)$$

where we have again used the ϵ -Cauchy inequality to extract the L^2 norms of the errors. Now, since K is integrable, the weights $w_i(K)$ are bounded which along with a simple real number inequality $(a+b)^2 \leq 2(a^2+b^2)$ yields a nonlocal recurrence

$$\delta \|e^n\|^2 \leq C \left(\rho(N, h)^2 + \|e^{n-1}\|^2 + \|e^{n-2}\|^2 + \sum_{i=0}^M \left(\|e^{n-1-i}\|^2 + \|e^{n-i-2}\|^2 \right) \right), \quad (115)$$

which, by changing the summation variable and enlarging the constant C , can be transformed into

$$\|e^n\|^2 \leq (1 + Ch) \|e^{n-1}\|^2 + Ch \sum_{i=2}^{M+1} \|e^{n-i}\|^2 + Ch \rho(N, h)^2. \quad (116)$$

Now, adding terms on both sides we can write

$$\|e^n\|^2 + Ch \sum_{i=1}^M \|e^{n-i}\|^2 \leq (1 + Ch) \left(\|e^{n-1}\|^2 + Ch \sum_{i=2}^{M+1} \|e^{n-i}\|^2 \right) + Ch \rho(N, h)^2. \quad (117)$$

Set

$$c_n := \|e^n\|^2 + Ch \sum_{i=1}^M \|e^{n-i}\|^2, \quad (118)$$

to obtain a simple recurrence

$$c_n \leq (1 + Ch) c_{n-1} + Ch \rho(N, h)^2. \quad (119)$$

By iteration we then have

$$\begin{aligned} c_n &\leq (1 + Ch)^{n-1} c_1 + Ch \rho(N, h)^2 \sum_{i=0}^n (1 + Ch)^i \\ &\leq (1 + Ch)^{n-1} c_1 + (1 + Ch)^{n+1} \rho(N, h)^2 \leq e^{Ct_0} (c_1 + \rho(N, h)^2), \end{aligned} \quad (120)$$

and therefore,

$$\|e^n\|^2 \leq C \left(\|e^1\|^2 + Ch \sum_{i=1}^M \|e^{1-i}\|^2 + \rho(N, h)^2 \right). \quad (121)$$

Now, we are left with estimating the error made in the first predictor-corrector step (92)-(93) since the sum above involves the initial condition. To this end, set $g^1 = W - R_N u^1$. Similarly as above we can show that for the predictor (92) we have

$$\delta \|g^1\|^2 \leq C \left(\|U^0 - u^{1-\theta}\|^2 + \rho(N, h)^2 \right). \quad (122)$$

Then,

$$\|U^0 - u^{1-\theta}\|^2 \leq \|e^0\|^2 + \|r^0\|^2 + Ch \leq C \left(\|e^0\|^2 + N^{-2m} + h \right), \quad (123)$$

and it follows that

$$\|g^1\|^2 \leq C \left(\|e^0\|^2 + h(N^{-2m} + h)^2 + h\rho(N, h)^2 \right). \quad (124)$$

Next, we move to the corrector stage (93) to obtain

$$\delta \|e^1\|^2 \leq C \left(\|\widehat{W}^{1-\theta} - u^{1-\theta}\|^2 + \rho(N, h)^2 \right). \quad (125)$$

Reasoning as above we have

$$\begin{aligned} \|\widehat{W}^{1-\theta} - u^{1-\theta}\| &\leq \|\widehat{g}^{1-\theta}\| + \|\widehat{R}_N u^{1-\theta} - u^{1-\theta}\| \leq \|e^0\| + \|g^1\| + \|\widehat{R}_N u^{1-\theta} - u^{1-\theta}\| \\ &\leq \|e^0\| + \|g^1\| + CN^{-2m} + \|\widehat{R}_N u^{1-\theta} - R_N u^{1-\theta}\|. \end{aligned} \quad (126)$$

Using the estimate on $\|g^1\|$ from the prediction stage we obtain

$$\begin{aligned} \|\widehat{W}^{1-\theta} - u^{1-\theta}\| &\leq C \left(\|e^0\| + h^{\frac{1}{2}}(N^{-2m} + h) + h^{\frac{1}{2}}\rho(N, h) + N^{-2m} + \rho(N, h) \right) \\ &\leq C \left(\|e^0\| + h^{\frac{3}{2}} + \rho(N, h) \right). \end{aligned} \quad (127)$$

Now, by going back to the estimate on the finite difference of the error we finally have

$$\|e^1\| \leq C \left(\|e^0\| + h^2 + \rho(N, h) \right). \quad (128)$$

The estimates on the initial value errors $\|e^{-i}\|$ where $i = 0, 1, 2, \dots, M$ follows from

$$\|e^{-i}\| = \|R_N u^{-i} - P_N \psi^{-i}\| \leq CN^{-2m}, \quad (129)$$

what ends the proof. \square

5 Implementation and numerical illustration

Now we are concerned about the practical use of the aforementioned algorithm and its efficient implementation. Let U^n be expanded into our basis (18)

$$U^n = \sum_{i=0}^N y_i^n \phi_i, \quad (130)$$

then, plugging into (90), by orthonormality of $\{\phi_i\}_i$ we obtain

$$\left(I + (1 - \theta)hA(\overline{U}^{n-\theta}) \right) \mathbf{y}^n = \left(I - \theta hA(\overline{U}^{n-\theta}) \right) \mathbf{y}^{n-1} + h \mathbf{f}_h(\overline{U}^{n-\theta}), \quad n \geq 2, \quad (131)$$

where $\mathbf{y}^n = \{y_i^n\}_{i=0}^N$ is a vector of solutions, while the stiffness matrix $A = \{A_{ij}\}_{i,j=0}^N$ and the load vector $\mathbf{f}_h = \{f_{h,i}\}_i$ are defined by

$$A_{ij} = (D(\overline{U}^{n-\theta}); \phi_i, \phi_j), \quad f_{h,i} = (f_h(\overline{U}^{n-\theta}), \phi_i). \quad (132)$$

In the linear case, the stiffness matrix is diagonal $A = \text{diag}(\lambda_i)_i$ with eigenvalues (19). The implementation requires solving (131) in each time step for \mathbf{y}^n which reduces to inverting the nonsingular

matrix $I + (1 - \theta)hA(\bar{U}^{n-\theta})$. For the linear diffusion, this matrix is constant over time and the inversion needs to be done only at the initialization phase.

We would like to numerically verify the above results concerning convergence. To this end we will calculate the order of the method for the Crank-Nicolson scheme with $\theta = 1/2$, with trapezoidal quadrature (86) and two choices of nonlocal operator kernels. The first one is the Gaussian as was suggested in the original work [5]

$$K(s) = G(s) := Ae^{-\frac{(\tau-2s)^2}{8\sigma^2}}, \quad (133)$$

where A is the amplitude and σ^2 is the variance. This kernel is responsible for a short memory effect due to exponential decay of its tail. In contrast to that, we can also consider a long memory kernel obtained by the power law describing heavy tail

$$K(s) = K_\alpha(s) = \frac{1}{\Gamma(\alpha)}s^{\alpha-1}, \quad \alpha > 0. \quad (134)$$

In the above, the prefactor involving gamma function has been chosen in order to be consistent with the Liouville fractional integral

$$I^\alpha y(t) = \frac{1}{\Gamma(\alpha)} \int_{-\infty}^t (t-s)^{\alpha-1} y(s) ds, \quad (135)$$

which arise after substitution $s \rightarrow t-s$ and allowing for the infinite memory with $\tau \rightarrow \infty$. Fractional integrals and fractional derivatives are important in many applications and there is a very vigorous research going on this topic: both applied and pure. They let us model a number of nonlocal phenomena such as dynamics in quantum optics [69], physics of plasma [15], movement of bacteria and amoeba [39], G-protein on cell surface [74], hydrology [13, 57, 58, 24, 60, 59], and motion of dislocations in crystal lattice [30]. Interested reader can find additional information in [50].

In our numerical examples we would like to test two cases: either linear diffusion with nonlocal operator or nonlinear diffusion without nonlocality. Errors are calculated in the L^2 norm and the coding is done in Julia programming language. We have implemented several performance mechanisms:

- All x -integrals are calculated using Gaussian quadrature with pregenerated Legendre weights.
- Where possible, we utilize parallel computing on several threads/cores (multi-threading). For example, stiffness matrix and load vector entries, as well as quadrature weights (85)-(86) can readily be calculated effectively in this way.
- Quadrature weights need only be generated once as soon as the kernel K and the step h are fixed.
- For linear diffusivity the stiffness matrix is pregenerated. For nonlinear diffusion we utilize multi-threading.

We have found that approach based on parallelism is highly efficient with respect to the single core calculations.

Below, for concreteness we set $\tau = 0.4$ and $t_0 = 0.5$. Moreover, the initial condition is always taken to be

$$\psi(x, s) = \frac{x^\mu}{1+s}, \quad (136)$$

where μ is a sufficiently large positive integer to ensure regularity of the initial condition. In our calculations we choose $\mu = 20$. Overall, we solve three cases of our problem

$$\begin{cases} D(u) = e^{-\beta u}, \\ f(x, t, u, w) = 1, \end{cases} \quad \begin{cases} D(u) = 1, \\ f(x, t, u, w) = w, \\ K(s) = G(s), \end{cases} \quad \begin{cases} D(u) = 1, \\ f(x, t, u, w) = w, \\ K(s) = K_\alpha(s), \end{cases} \quad (137)$$

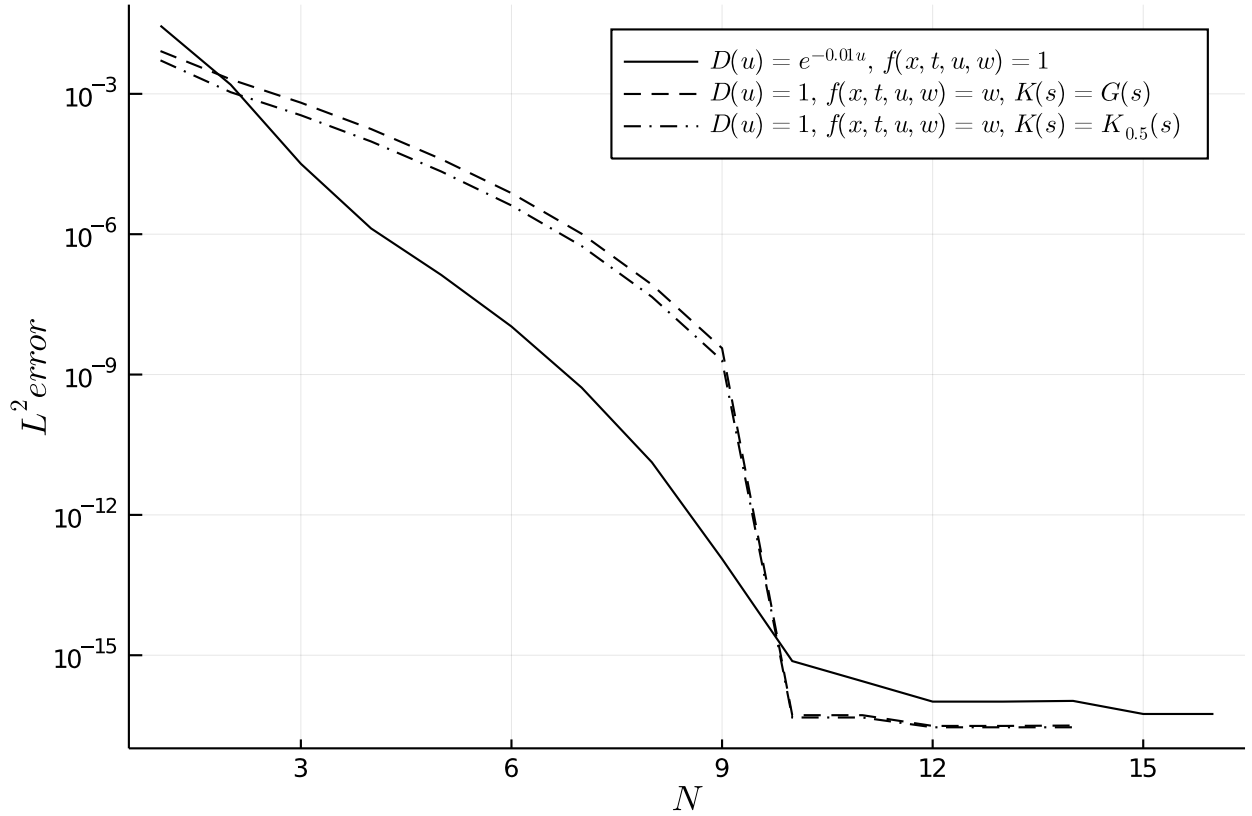


Figure 1: Numerically calculated L^2 error between solutions with $N_{max} = 30$ for different N and problems given in (137).

which test effects of nonlinearity and nonlocality.

First, in order to check the spectral accuracy of the spatial discretization we fix the time step to be $h = 2 \times 10^{-2}$ and compare solutions obtained for different N with the one calculated for $N_{max} = 30$. The latter is treated as „exact”. The comparison is done at $t = 0.125$ in order to not let diffusive effects to force the solution to decay which can happen for larger times. Results of our simulations are shown in Fig. 1 where a semilog plot of errors is presented. As we can see, the spectral accuracy is confirmed for all considered cases. The error saturates at machine epsilon for $N \approx 10$ for all problems. Regardless the kernel for nonlocal operator, the plots are similar. The error could be made even smaller if we decreased the time step, however, we wanted to clearly show the error trend.

The temporal order is calculated in a similar way. Here, we use $N = N_{max} = 15$ which is based on our previous finding that spectral accuracy is achieved for N of order of 10. Our „exact” solution is then precalculated for $h_{min} = 0.2 \times 10^{-2}$ and compared with calculations done with larger steps. The time of comparison is taken to be t_0 . In Fig. 2 we present the log-log plot of L^2 error for different values of h . As we can see, for all considered cases the order of convergence is confirmed to be equal to 2, that is the lines are parallel to h^2 for large values of h^{-1} (small h). Note that the weakly-singular kernel in the fractional integral (134) does not impair the accuracy. This is because we have chosen to integrate the kernel *exactly* using the product integration rule.

6 Conclusion

Motivated by the efficient use of spectral method for solving equations of energy balance models we have provided convergence proofs for Galerkin-Legendre scheme. Discretization in time using

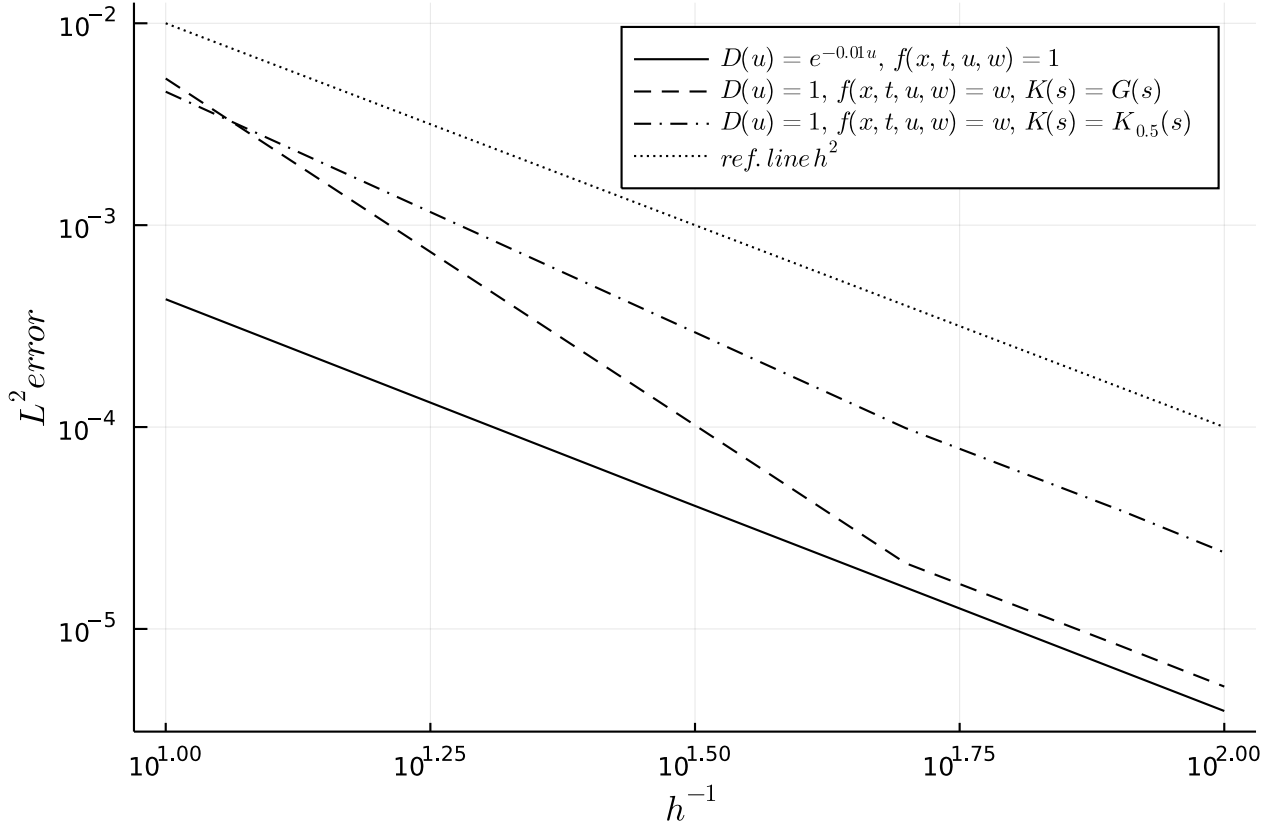


Figure 2: Numerically calculated L^2 error between solutions with $h_{min} = 0.2 \times 10^{-2}$ for different h and problems given in (137).

extrapolated coefficients granted a linear second order method that can quickly calculate the solution to the required accuracy. Moreover, using a parallelized code fragments helped to improve the performance even further. Due to the nonlocal operator, that requires to take into account the history of the evolution, the initial computational cost of the simulations can be high. Thanks to spectral accuracy and multi-thread computations we were able to reduce it. In future work we will extend our method to some more general equations with nonlocal specific heat and diffusivity proportional to the gradient.

Acknowledgement

Ł.P. has been supported by the National Science Centre, Poland (NCN) under the grant Sonata Bis with a number NCN 2020/38/E/ST1/00153.

References

- [1] Kendall Atkinson, David Chien, and Olaf Hansen. A spectral method for nonlinear elliptic equations. *Numerical Algorithms*, 74(3):797–819, 2017.
- [2] Dumitru Baleanu, Kai Diethelm, Enrico Scalas, and Juan J Trujillo. *Fractional calculus: models and numerical methods*, volume 3. World Scientific, 2012.

- [3] R Bermejo, Jaime Carpio, JI Díaz, and P Galan Del Sastre. A finite element algorithm of a nonlinear diffusive climate energy balance model. *Pure and Applied Geophysics*, 165(6):1025–1047, 2008.
- [4] Rodolfo Bermejo, Jaime Carpio, Jesús Ildefonso Diaz, and L Tello. Mathematical and numerical analysis of a nonlinear diffusive climate energy balance model. *Mathematical and computer modelling*, 49(5-6):1180–1210, 2009.
- [5] K Bhattacharya, M Ghil, and IL Vulis. Internal variability of an energy-balance model with delayed albedo effects. *Journal of Atmospheric Sciences*, 39(8):1747–1773, 1982.
- [6] Mikhail I Budyko. The effect of solar radiation variations on the climate of the earth. *Tellus*, 21(5):611–619, 1969.
- [7] Piermarco Cannarsa, Martina Malfitana, and Patrick Martinez. Parameter determination for energy balance models with memory. In *Mathematical Approach to Climate Change and its Impacts*, pages 83–130. Springer, 2020.
- [8] JR Cannon and Yanping Lin. A priori l^2 error estimates for finite-element methods for nonlinear diffusion equations with memory. *SIAM Journal on Numerical Analysis*, 27(3):595–607, 1990.
- [9] Claudio Canuto, M Yousuff Hussaini, Alfio Quarteroni, and Thomas A Zang. *Spectral methods: fundamentals in single domains*. Springer Science & Business Media, 2007.
- [10] Martin Claussen, L Mysak, A Weaver, Michel Crucifix, Thierry Fichefet, M-F Loutre, Shlomo Weber, Joseph Alcamo, Vladimir Alexeev, André Berger, et al. Earth system models of intermediate complexity: closing the gap in the spectrum of climate system models. *Climate dynamics*, 18(7):579–586, 2002.
- [11] WD Collins, V Ramaswamy, M Dan Schwarzkopf, Ying Sun, Robert W Portmann, Q Fu, SEB Casanova, J-L Dufresne, David W Fillmore, PMD Forster, et al. Radiative forcing by well-mixed greenhouse gases: Estimates from climate models in the intergovernmental panel on climate change (ipcc) fourth assessment report (ar4). *Journal of Geophysical Research: Atmospheres*, 111(D14), 2006.
- [12] Michel Crucifix. Oscillators and relaxation phenomena in pleistocene climate theory. *Phil. Trans. R. Soc. A*, 370(1962):1140–1165, 2012.
- [13] Arturo de Pablo, Fernando Quiros, Ana Rodriguez, and Juan Luis Vazquez. A fractional porous medium equation. *Advances in Mathematics*, 226(2):1378–1409, 2011.
- [14] Bernard De Saedeleer, Michel Crucifix, and Sebastian Wiczorek. Is the astronomical forcing a reliable and unique pacemaker for climate? a conceptual model study. *Climate Dynamics*, 40(1-2):273–294, 2013.
- [15] Diego del Castillo-Negrete, BA Carreras, and VE Lynch. Nondiffusive transport in plasma turbulence: a fractional diffusion approach. *Physical Review Letters*, 94(6):065003, 2005.
- [16] Jesús Ildefonso Díaz. On the mathematical treatment of energy balance climate models. In *The mathematics of models for climatology and environment*, pages 217–251. Springer, 1997.
- [17] JI Díaz. On a free boundary problem arising in climatology. *Free Boundary Problems: Theory and Applications*, (N. Kenmochi, ed.), 2:92–109, 2000.

- [18] JI Diaz, G Hetzer, and L Tello. An energy balance climate model with hysteresis. *Nonlinear Analysis: Theory, Methods & Applications*, 64(9):2053–2074, 2006.
- [19] JI Diaz, A Hidalgo, and L Tello. Multiple solutions and numerical analysis to the dynamic and stationary models coupling a delayed energy balance model involving latent heat and discontinuous albedo with a deep ocean. *Proceedings of the Royal Society A: Mathematical, Physical and Engineering Sciences*, 470(2170):20140376, 2014.
- [20] JI Díaz, JA Langa, and J Valero. On the asymptotic behaviour of solutions of a stochastic energy balance climate model. *Physica D: Nonlinear Phenomena*, 238(9-10):880–887, 2009.
- [21] Kai Diethelm and Neville J Ford. Analysis of fractional differential equations. *Journal of Mathematical Analysis and Applications*, 265(2):229–248, 2002.
- [22] Peter D Ditlevsen and Peter Ashwin. Complex climate response to astronomical forcing: The middle-pleistocene transition in glacial cycles and changes in frequency locking. *Frontiers in Physics*, 6:62, 2018.
- [23] Jim Douglas and Todd Dupont. Galerkin methods for parabolic equations with nonlinear boundary conditions. *Numerische Mathematik*, 20(3):213–237, 1973.
- [24] Abd El-Ghany El Abd and Jacek J Milczarek. Neutron radiography study of water absorption in porous building materials: anomalous diffusion analysis. *Journal of Physics D: Applied Physics*, 37(16):2305, 2004.
- [25] AC Fowler. A simple thousand-year prognosis for oceanic and atmospheric carbon change. *Pure and Applied Geophysics*, 172(1):49–56, 2015.
- [26] AC Fowler, REM Rickaby, and EW Wolff. Exploration of a simple model for ice ages. *GEM-International Journal on Geomathematics*, 4(2):227–297, 2013.
- [27] Andrew Fowler. *Mathematical geoscience*, volume 36. Springer Science & Business Media, 2011.
- [28] Michael Ghil and Hervé Le Treut. A climate model with cryodynamics and geodynamics. *Journal of Geophysical Research: Oceans*, 86(C6):5262–5270, 1981.
- [29] Charles E Graves, Wan-Ho Lee, and Gerald R North. New parameterizations and sensitivities for simple climate models. *Journal of Geophysical Research: Atmospheres*, 98(D3):5025–5036, 1993.
- [30] AK Head. Dislocation group dynamics iii. similarity solutions of the continuum approximation. *Philosophical Magazine*, 26(1):65–72, 1972.
- [31] Isaac M Held and Max J Suarez. Simple albedo feedback models of the icecaps. *Tellus*, 26(6):613–629, 1974.
- [32] Georg Hetzer. A functional reaction-diffusion equation from climate modeling: S-shapedness of the principal branch of fixed points of the time-1-map. *Differential and Integral equations*, 8(5):1047–1059, 1995.
- [33] Georg Hetzer. Global existence, uniqueness, and continuous dependence for a reaction-diffusion equation with memory. *Electronic Journal of Differential Equations*, 1996(05):1–16, 1996.
- [34] Georg Hetzer. A quasilinear functional reaction-diffusion equation from climate modeling. *Nonlinear Analysis: Theory, Methods & Applications*, 30(5):2547–2556, 1997.

- [35] Arturo Hidalgo and Lourdes Tello. On a climatological energy balance model with continents distribution. *Discrete & Continuous Dynamical Systems-A*, 35(4):1503, 2015.
- [36] Arturo Hidalgo and Lourdes Tello. Numerical approach of the equilibrium solutions of a global climate model. *Mathematics*, 8(9):1542, 2020.
- [37] E Källén, C Crafoord, and M Ghil. Free oscillations in a climate model with ice-sheet dynamics. *Journal of the Atmospheric Sciences*, 36(12):2292–2303, 1979.
- [38] Marie-Noëlle Le Roux and Vidar Thomée. Numerical solution of semilinear integrodifferential equations of parabolic type with nonsmooth data. *SIAM Journal on Numerical Analysis*, 26(6):1291–1309, 1989.
- [39] M Levandowsky, BS White, and FL Schuster. Random movements of soil amebas. *Acta Protozoologica*, 36:237–248, 1997.
- [40] Changpin Li and Fanhai Zeng. *Numerical methods for fractional calculus*, volume 24. CRC Press, 2015.
- [41] MS Lian and Robert D Cess. Energy balance climate models: A reappraisal of ice-albedo feedback. *Journal of the Atmospheric Sciences*, 34(7):1058–1062, 1977.
- [42] Charles A Lin. The effect of nonlinear diffusive heat transport in a simple climate model. *Journal of the Atmospheric Sciences*, 35(2):337–340, 1978.
- [43] Peter Linz. *Analytical and numerical methods for Volterra equations*, volume 7. Siam, 1985.
- [44] Wenjie Liu, Jiebao Sun, and Boying Wu. Space-time spectral method for two-dimensional semilinear parabolic equations. *Mathematical Methods in the Applied Sciences*, 39(7):1646–1661, 2016.
- [45] Mitchell Luskin. A galerkin method for nonlinear parabolic equations with nonlinear boundary conditions. *SIAM Journal on Numerical Analysis*, 16(2):284–299, 1979.
- [46] Kirk A Maasch and Barry Saltzman. A low-order dynamical model of global climatic variability over the full pleistocene. *Journal of Geophysical Research: Atmospheres*, 95(D2):1955–1963, 1990.
- [47] Richard McGehee and Clarence Lehman. A paleoclimate model of ice-albedo feedback forced by variations in earth’s orbit. *SIAM Journal on Applied Dynamical Systems*, 11(2):684–707, 2012.
- [48] Richard McGehee and Esther Widiasih. A quadratic approximation to budyko’s ice-albedo feedback model with ice line dynamics. *SIAM Journal on Applied Dynamical Systems*, 13(1):518–536, 2014.
- [49] Kendal McGuffie and Ann Henderson-Sellers. *A climate modelling primer*. John Wiley & Sons, 2005.
- [50] Ralf Metzler and Joseph Klafter. The random walk’s guide to anomalous diffusion: a fractional dynamics approach. *Physics reports*, 339(1):1–77, 2000.
- [51] Gerald R North. Analytical solution to a simple climate model with diffusive heat transport. *Journal of Atmospheric Sciences*, 32(7):1301–1307, 1975.
- [52] Gerald R North. Theory of energy-balance climate models. *Journal of Atmospheric Sciences*, 32(11):2033–2043, 1975.

- [53] Gerald R North, Robert F Cahalan, and James A Coakley Jr. Energy balance climate models. *Reviews of Geophysics*, 19(1):91–121, 1981.
- [54] Gerald R North and James A Coakley Jr. Differences between seasonal and mean annual energy balance model calculations of climate and climate sensitivity. *Journal of Atmospheric Sciences*, 36(7):1189–1204, 1979.
- [55] Gerald R North and Kwang-Yul Kim. *Energy Balance Climate Models*. John Wiley & Sons, 2017.
- [56] Karl HM Nyman and Peter D Ditlevsen. The middle pleistocene transition by frequency locking and slow ramping of internal period. *Climate Dynamics*, pages 1–16, 2019.
- [57] Yakov Pachepsky, Dennis Timlin, and Walter Rawls. Generalized richards’ equation to simulate water transport in unsaturated soils. *Journal of Hydrology*, 272(1):3–13, 2003.
- [58] Łukasz Płociniczak. Approximation of the Erdélyi–Kober operator with application to the time-fractional porous medium equation. *SIAM Journal on Applied Mathematics*, 74(4):1219–1237, 2014.
- [59] Łukasz Płociniczak. Derivation of the nonlocal pressure form of the fractional porous medium equation in the hydrological setting. *Communications in Nonlinear Science and Numerical Simulation*, 76:66–70, 2019.
- [60] Łukasz Płociniczak. Numerical method for the time-fractional porous medium equation. *SIAM Journal on Numerical Analysis*, 57(2):638–656, 2019.
- [61] Łukasz Płociniczak. Asymptotic analysis of internal relaxation oscillations in a conceptual climate model. *IMA Journal of Applied Mathematics*, 85(3):467–494, 2020.
- [62] Łukasz Płociniczak. Hopf bifurcation in a conceptual climate model with ice–albedo and precipitation–temperature feedbacks. *Nonlinear Analysis: Real World Applications*, 51:102967, 2020.
- [63] Courtney Quinn, Jan Sieber, and Anna S von der Heydt. Effects of periodic forcing on a paleoclimate delay model. *SIAM Journal on Applied Dynamical Systems*, 18(2):1060–1077, 2019.
- [64] Courtney Quinn, Jan Sieber, Anna S von der Heydt, and Timothy M Lenton. The mid-pleistocene transition induced by delayed feedback and bistability. *Dynamics and Statistics of the Climate System*, 3(1):dzy005, 2018.
- [65] David A Randall, Richard A Wood, Sandrine Bony, Robert Colman, Thierry Fichefet, John Fyfe, Vladimir Kattsov, Andrew Pitman, Jagadish Shukla, Jayaraman Srinivasan, et al. Climate models and their evaluation. In *Climate change 2007: The physical science basis. Contribution of Working Group I to the Fourth Assessment Report of the IPCC (FAR)*, pages 589–662. Cambridge University Press, 2007.
- [66] Andrew W Robertson and Michael Ghil. Solving problems with gcms: General circulation models and their role in the climate modeling hierarchy. 2000.
- [67] Lionel Roques, Mickaël D Chekroun, Michel Cristofol, Samuel Soubeyrand, and Michael Ghil. Parameter estimation for energy balance models with memory. *Proceedings of the Royal Society A: Mathematical, Physical and Engineering Sciences*, 470(2169):20140349, 2014.

- [68] Barry Saltzman. *Dynamical paleoclimatology: generalized theory of global climate change*, volume 80. Academic Press, 2002.
- [69] Stefan Schaufler, WP Schleich, and VP Yakovlev. Scaling and asymptotic laws in subrecoil laser cooling. *EPL (Europhysics Letters)*, 39(4):383, 1997.
- [70] William D Sellers. A global climatic model based on the energy balance of the earth-atmosphere system. *Journal of Applied Meteorology*, 8(3):392–400, 1969.
- [71] Jie Shen, Tao Tang, and Li-Lian Wang. *Spectral methods: algorithms, analysis and applications*, volume 41. Springer Science & Business Media, 2011.
- [72] Thomas Stocker. Model hierarchy and simplified climate models. In *Introduction to Climate Modelling*, pages 25–51. Springer, 2011.
- [73] Peter H Stone. The effect of large-scale eddies on climatic change. *Journal of Atmospheric Sciences*, 30(4):521–529, 1973.
- [74] Titiwat Sungkaworn, Marie-Lise Jobin, Krzysztof Burnecki, Aleksander Weron, Martin J Lohse, and Davide Calebiro. Single-molecule imaging reveals receptor–g protein interactions at cell surface hot spots. *Nature*, 550(7677):543, 2017.
- [75] Vidar Thomée. *Galerkin finite element methods for parabolic problems*, volume 25. Springer Science & Business Media, 2007.
- [76] Aleksandr Filippovich Timan. *Theory of approximation of functions of a real variable*. Elsevier, 2014.
- [77] Jacques Tort and Judith Vancostenoble. Determination of the insolation function in the non-linear sellers climate model. *Annales de l’Institut Henri Poincaré (C) Non Linear Analysis*, 29(5):683–713, 2012.
- [78] Eli Tziperman, Maureen E Raymo, Peter Huybers, and Carl Wunsch. Consequences of pacing the pleistocene 100 kyr ice ages by nonlinear phase locking to milankovitch forcing. *Paleoceanography and Paleoclimatology*, 21(4), 2006.
- [79] James Walsh and Esther Widiasih. A dynamics approach to a low-order climate model. *Discrete & Continuous Dynamical Systems-B*, 19(1):257, 2014.
- [80] James Walsh, Esther Widiasih, Jonathan Hahn, and Richard McGehee. Periodic orbits for a discontinuous vector field arising from a conceptual model of glacial cycles. *Nonlinearity*, 29(6):1843, 2016.
- [81] Mary Fanett Wheeler. A priori l_2 error estimates for galerkin approximations to parabolic partial differential equations. *SIAM Journal on Numerical Analysis*, 10(4):723–759, 1973.
- [82] Esther R Widiasih. Dynamics of the budyko energy balance model. *SIAM Journal on Applied Dynamical Systems*, 12(4):2068–2092, 2013.
- [83] Xiangsheng Xu. Existence and regularity theorems for a free boundary problem governing a simple climate model. *Applicable Analysis*, 42(1-4):33–57, 1991.